

REDUCTIVE DISSOLUTION KINETICS OF Al-SUBSTITUTED GOETHITES

ESTELA GONZALEZ, MARÍA C. BALLESTEROS AND ELSA H. RUEDA*

Departamento de Química e Ingeniería Química, Universidad Nacional del Sur, Av. Alem 1253 8000 - Bahía Blanca, Argentina

Abstract—Several Al-substituted goethites were synthesized by hydrolysis of Fe^{3+} salt solutions. The kinetics of the reductive dissolution of these goethites in dithionite-ethylenediaminetetra acetic acid (D-EDTA) was studied at pH 5.5, at 303, 323 and 333 K. The initial dissolution rate (R) per unit of surface area decreases with Al substitution. In the sample with greater Al content (G''_7), the kinetic profiles of the dissolved Fe fraction vs. time gave a small positive intercept. The kinetic profile of R as a function of EDTA initial concentration shows a significant weakening in the presence of Al. The maximum is flatter and wider in Al-substituted goethite than that of pure goethite. In sample G''_7 , where the Al content is 11.3 mol.% the maximum is obtained when the [D]:[EDTA] initial ratio is ~4.5 vs. 2 in un-substituted goethite. These results can be attributed to the lesser density of the more active dimeric sites, the presence of more strongly bonded $\text{Al}-\text{O}-\text{Fe}$ with regard to $\text{Fe}-\text{O}$ and the small value for the $\equiv \text{Al}-\text{EDTA}$ surface species constant. Activation energy (E_a) increases with Al substitution. Its value is doubled from G_0 (pure goethite) to G''_7 (11.3 mol.% of Al). The frequency factor (A) acts in the opposite sense to E_a , but it is not sufficient to outweigh the effect of E_a .

Key Words—Al Substitution, Dithionite-EDTA, Iron Oxide, Reductive Dissolution.

INTRODUCTION

Goethite is the best example of an isomorphously substituted Fe oxide, and of the various possible substituents in both natural and synthetic samples, Al is the best known example. One reason for this is the ubiquity and abundance of Al in soils and rocks and its mobilization, together with Fe, during weathering (Cornell and Schwertmann, 1996).

The substitution of Fe^{3+} by Al^{3+} has been reported both in natural and synthetic goethites (Norrish and Taylor, 1961; Mendelovici *et al.*, 1979; Lewis and Schwertmann, 1979a,b; Schulze, 1984; Mann *et al.*, 1985; Schulze and Schwertmann, 1987; Wolska *et al.* 1992a,b).

The ionic substitution of Al for Fe in the structure of goethite has a marked effect on goethite properties. In fact, variations in crystal size, shape and surface area, infrared (IR) spectra, X-ray diffraction (XRD) patterns, structural OH content, thermal and magnetic properties and dissolution behavior were observed in earlier works (Murad and Schwertmann, 1983; Schulze and Schwertmann, 1984; Schwertmann, 1984; Schulze and Schwertmann, 1987; Cambier, 1986; Torrent *et al.*, 1987; Pollard *et al.*, 1991; Jeanroy *et al.*, 1991; Hazemann *et al.*, 1991).

The dissolution process is usually considered to take place in steps which are analogous to those in the reverse process of crystal growth. Dissolution, however, is not simply the reverse of crystal growth. Goethite, for example, may dissolve by proton attack, by the action of complexing ions, and reductively, and each process follows a different mechanism (Blesa *et al.*, 1994).

The rate of dissolution of Fe oxides is affected by the properties of the overall system (*e.g.* temperature, UV light), the composition of the solution phase (*e.g.* redox potential, concentration of acids, concentration of reductants and complexing agents) and the properties of the oxide (*e.g.* stoichiometry, crystal chemistry, crystal habit, surface roughness, surface morphology and presence of guest ions).

Dissolution kinetics may provide an indication of the effects of Al substitution on the solubility and stability of the Fe oxides in the soil environment. Acid dissolution of metal-substituted goethite and hematite was studied by Schwertmann and Latham (1986), Lim-Nunez and Gilkes (1987), Ruan and Gilkes (1995) and Wells *et al.* (2001). In natural environments, reductive dissolution is by far the most common dissolution mechanism. The reductive dissolution by Na dithionite of several goethites and hematites of different Al-substitution levels was investigated by Torrent *et al.* (1987). They suggested that the main reason for the preferential dissolution of hematite in natural environments is its lower Al substitution.

In a previous paper (Rueda *et al.*, 1992) the method of Mehra and Jackson (1960) was optimized in the synthetic goethite dissolution using EDTA as the complexing agent at 315 K and pH 5.5. This paper reports the results of a study of reductive dissolution of a range of Al-substituted goethites applying the method mentioned above. The reductive dissolution rate of substituted goethite containing 11.3 mol.% Al as a function of EDTA concentration was also studied in this work. The comparison of these data with those obtained earlier for pure goethite offers an insight into the relative contributions of the possible pathways of dissolution. Activation energy and frequency factor

* E-mail address of corresponding author:
ehrueda@criba.edu.ar

values for substituted goethites were derived from the Arrhenius equation and related to the substitution level.

MATERIALS AND METHODS

Series of Al-substituted goethites were prepared in hydrothermal conditions following the method described by Schwertmann and Cornell (1991). Different amounts of aluminate solution prepared by addition of 500 cm^3 of $0.5 \text{ mol} \cdot \text{dm}^{-3}$ $\text{Al}(\text{NO}_3)_3$ solution to 300 cm^3 of $5.0 \text{ mol} \cdot \text{dm}^{-3}$ KOH solution with constant stirring, were poured into a 2 dm^3 polyethylene flask and mixed with 165 cm^3 of $5.0 \text{ mol} \cdot \text{dm}^{-3}$ KOH. Then, 100 cm^3 of $0.5 \text{ mol} \cdot \text{dm}^{-3}$ $\text{Fe}(\text{NO}_3)_3$ solution were added quickly to each bottle. Immediately all the suspensions were diluted to 2 dm^3 with twice distilled water. The bottles were then sealed, the suspension mixed thoroughly and placed into an air oven at 343 K for ~14 days. After the required period, during which the suspensions were periodically shaken briefly by hand, they were centrifuged and the products washed twice with 400 cm^3 of $1.0 \text{ mol} \cdot \text{dm}^{-3}$ KOH to remove extra Al, adjusting the pH to 7.5 with HCl, to allow maximum flocculation and efficient removal of soluble material with negligible loss of solid phase. Finally, the samples were washed and dried in oven at 323 K, crushed and stored in glass vials for later analysis.

Aluminum in the system favors hematite over goethite formation. To avoid the presence of hematite in the samples with higher Al content, they were aged at lower temperatures and for longer periods of time.

All subsequent measurements were carried out on the material remaining after oxalate extraction. Oxalate-extractable Fe (Fe_{o}) was determined after treatment with NH_4 oxalate at pH 3, in the dark, for 4 h (McKeague and Day, 1966).

The chemical composition of the samples was determined by dissolving 100 mg of solid in 20 cm^3 of $6.0 \text{ mol} \cdot \text{dm}^{-3}$ HCl at 333–353 K. The Fe and Al contents were determined using a GBC 932 atomic adsorption spectrophotometer (AAS).

X-ray diffraction (XRD) patterns were obtained using a Rigaku Denki Max-IIIC diffractometer, equipped with graphite monochromator, $\text{CuK}\alpha$ radiation (35 kV, 15 mA) at scan rate of $1^\circ 2\theta/\text{min}$. Specimens for scanning electronic microscopy (SEM) were dispersed in bidistilled water with ultrasonic treatment and a drop of suspension was placed onto a metallic support. The SEM images were obtained using a Philips SEM 515 device operated at 30 keV. Specific surface areas were determined by the BET- N_2 multipoint adsorption method in a Micromeritics, Accusorb 2100 E, outgassing the samples at 323 K.

All the kinetic experiments were performed over samples in which goethite was the only phase present. Dissolution experiments were carried out in a cylind-

rical Pyrex vessel encased in a thermostated water jacket. An EDTA solution at pH 5.5 was degassed by bubbling N_2 (which first passed through pyrogallol and water trap) for 30 min. Next, the desired amount of solid Na dithionite ($\text{Na}_2\text{S}_2\text{O}_4$) was added and the dissolution started by pouring the solid sample into the solution. During the experiments, particles were kept in suspension by means of a magnetic stirrer. The experiments to study the influence of ligand concentration were carried out at 303 K. To determine E_a , dissolution kinetics were measured at three temperatures (303, 323 and 333 K).

The kinetic behavior was recorded from the amount of Fe released. For that, aliquots of the dispersions were withdrawn at regular intervals and filtered through a $0.22 \mu\text{m}$ membrane. The amounts of dissolved Fe were determined by atomic absorption spectroscopy (AAS). Sample duplicates and blanks were included as a check on the reliability of the data. To eliminate the possible contribution of small particles to our measured ‘dissolved Fe’, some experiments were ended by quenching the reaction with alkaline thioglycollate (Baumgartner *et al.*, 1983), filtering off the solid through a $0.10 \mu\text{m}$ membrane. Both procedures yielded the same results.

RESULTS

Properties of Al-substituted goethites

The effects of preliminary treatment on the properties of the final product are listed in Table 1. At 343 K, XRD patterns showed an increase in the amount of hematite with increase in Al substitution. Schwertmann *et al.* (2000) suggested that the strong hematite-promoting effect of Al appears to be the result of a lower solubility of the Al-containing ferrihydrite precursor relative to pure ferrihydrite. Pure goethites of reasonably high Al substitution could be formed at lower temperatures (see samples G'_5 and G''_7 in Table 1). This indicates that the goethite crystals can accommodate more Al if they grow slowly than if they grow quickly. Since the rate of crystal growth decreases with the decrease in temperature, longer incubation times were necessary in these samples.

Although the XRD patterns were obtained in the range $2^\circ < 2\theta < 70^\circ$, in Figure 1 only the range $40^\circ < 2\theta < 70^\circ$ is shown to visualize better the displacement of the X-ray lines of Al-substituted goethites towards the higher angles due to Al-for-Fe substitution.

The $\text{Fe}_{\text{o}}/\text{Fe}_{\text{t}}$ ratio increased with Al addition, indicating that high Al content inhibits the transformation of ferrihydrite to crystalline forms.

The specific surface area of the Al-substituted goethites first decreased slightly as Al increased from 0 to 7 mol.% and then increased at higher Al substitutions. We did not find a clear trend between Al content and surface area, in agreement with Schulze and Schwertmann (1987) and Strauss *et al.* (1997).

Table 1. Synthesis conditions, composition and characteristics of the Al-substituted samples.

Sample	Synthesis temperature (K)	Al in initial solution (mol.%)	Al in solid phase (mol.%)	Crystalline phase	BET Surface area ($\text{m}^2 \text{g}^{-1}$)	$\text{Fe}_0/\text{Fe}_t^1$
G_0	343	—	—	$\alpha\text{-FeOOH}$	25.3	—
G_m	343	1.5	0.3	$\alpha\text{-FeOOH}$	24.7	—
G_1	343	3.0	0.8	$\alpha\text{-FeOOH}$	24.5	—
G_2	343	5.8	2.0	$\alpha\text{-FeOOH}$	23.9	—
G_4	343	11.0	3.7	$\alpha\text{-FeOOH}$	27.7	0.009
G_5	343	20.0	8.1	$\alpha\text{-FeOOH}$ $\alpha\text{-Fe}_2\text{O}_3$	n.d. ²	n.d.
G'_5	323	20.0	8.3	$\alpha\text{-FeOOH}$	29.7	0.016
G_7	343	27.0	11.1	$\alpha\text{-FeOOH}$ $\alpha\text{-Fe}_2\text{O}_3$	n.d.	n.d.
G'_7	323	27.0	11.2	$\alpha\text{-FeOOH}$ $\alpha\text{-Fe}_2\text{O}_3$	n.d.	n.d.
G''_7	310	27.0	11.3	$\alpha\text{-FeOOH}$	26.7	0.159

¹ Fe_0/Fe_t : ratio of oxalate-extractable Fe (Fe_0) to total Fe (Fe_t)² n.d.: not determined

—: not detected

The goethite crystals become smaller as Al substitution increases (Figure 2) and they change from large polydomainic crystals to smaller monodomainic ones according to Schulze and Schwertmann (1987).

Kinetics of reductive dissolution

The kinetic profiles of the fractions of dissolved Fe vs. time were deceleratory in samples with lower levels of Al substitution and essentially linear at higher Al

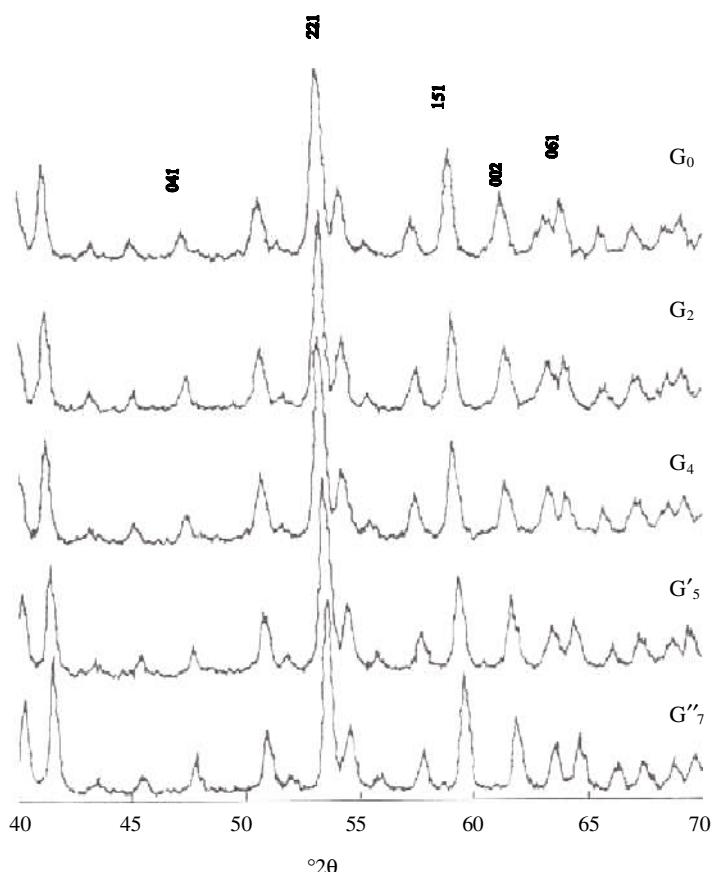


Figure 1. X-ray diffraction patterns of Al-substituted goethites.

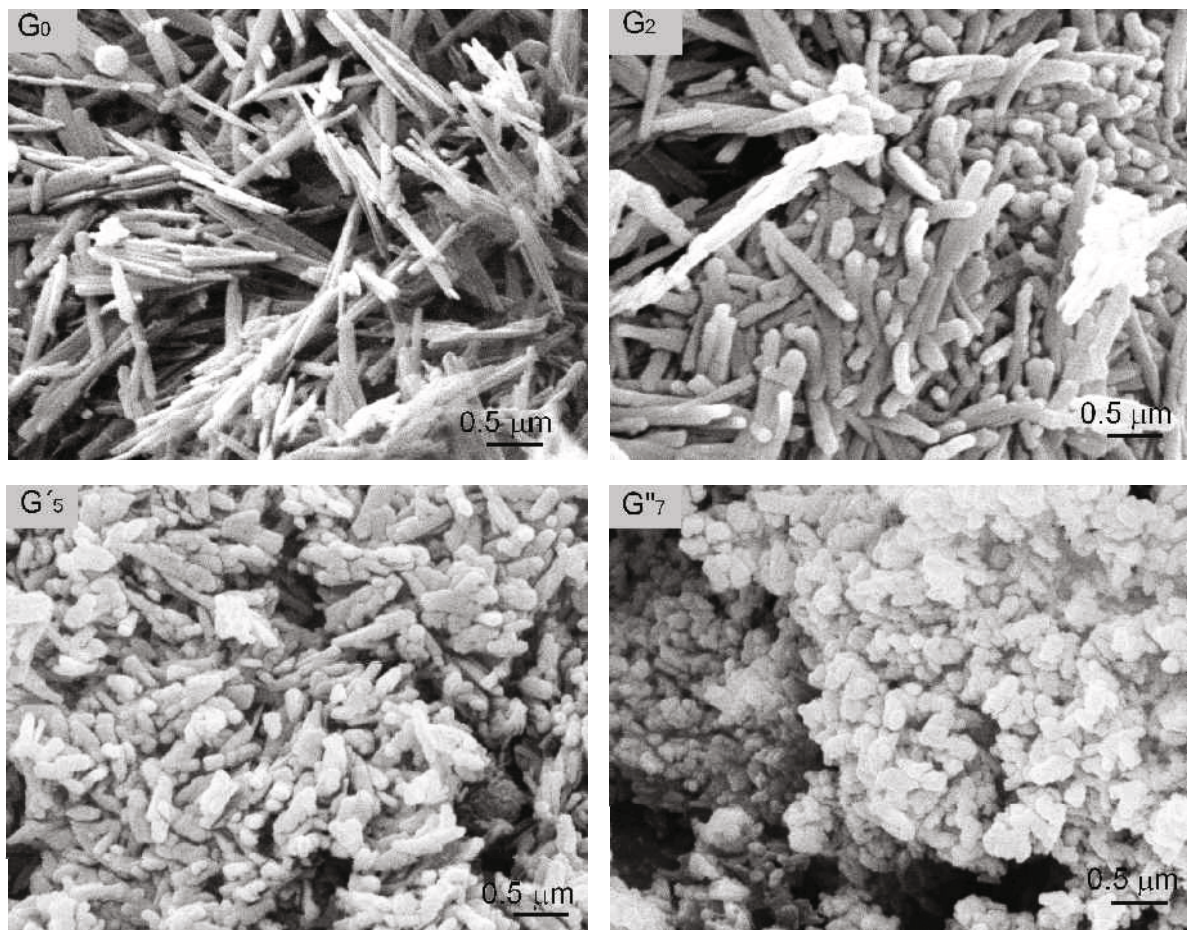


Figure 2. SEM images of three samples. G_0 , Goethite; G_2 , Al-goethite (2.0 mol.% Al); G'_5 (8.3 mol.% Al); G''_7 , Al-goethite (11.3 mol.% Al).

contents. Figure 3a shows the kinetic profiles of the different samples at 303 K and Figure 3b at 333 K. The initial dispersion observed in some substituted goethites at the lower temperature could have arisen through the presence of more reactive sites from structural defects.

We have chosen to discuss the kinetic behavior in terms of the initial rates, R , measured as the slope of df/dt vs. time in the initial near-linear region of the dissolution plots. In a previous study (Rueda *et al.*, 1992) we discussed the disadvantages that this system presents when we attempted to apply the contracting geometry rate law.

The dependence of R on the EDTA concentration, carried out on sample G''_7 , is shown in Figure 4b. These results are compared to those of the theoretical model applied to pure goethite in the same conditions (Rueda *et al.*, 1992) (Figure 4a). We observed that the rate in Al-substituted goethite diminishes with regard to un-substituted goethite and the kinetic profiles presents a maximum which is less sharp and shifted at higher ligand concentrations (an amplified scale was employed for a better appreciation of the maximum in G''_7). In

sample G''_7 the maximum is found when the $[D]:[EDTA]$ ratio is ~4.5. In un-substituted goethite this ratio is 2.

The dependence of $\ln R$ on the Al content at 303, 323 and 333 K is observed in Figure 5. The dissolution rate decreases with the substitution level, this effect is stronger at lower temperatures.

The temperature dependence of each sample is shown in the Arrhenius plot of Figure 6 and apparent E_a values for all samples can be calculated. The results are shown in Table 2 and Figure 7. The increase of E_a with Al substitution is clear; the E_a value in G''_7 is approximately twice that in G_0 .

DISCUSSION

Influence of Al substitution on the dissolution rate

The influence of Al substitution on the structural characteristics of synthetic goethites was previously studied in detail. The replacement of Fe^{3+} by the smaller Al^{3+} leads to slightly smaller unit-cell edge lengths. A linear relationship exists between the extent of Al substitution and the b and c edge lengths according to

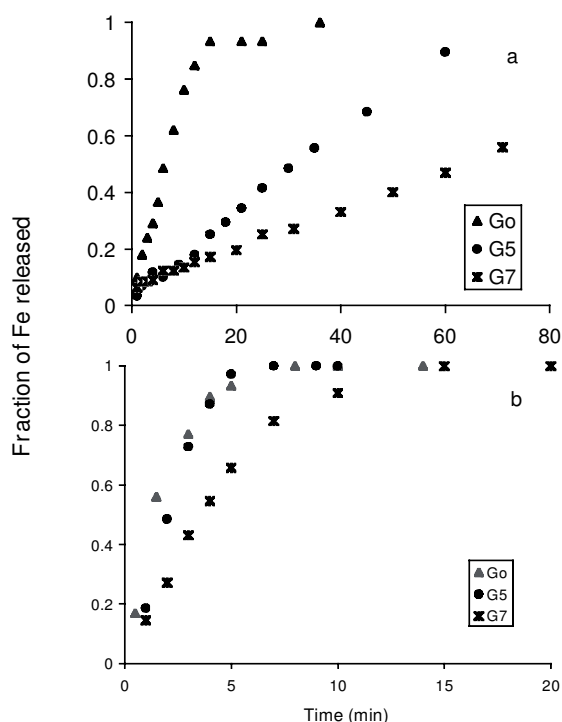


Figure 3. Fraction of total Fe released from goethite as a function of time for different Al contents; pH 5.5; [EDTA] 0.01 mol.dm⁻³; [S₂O₄²⁻] 5.75 × 10⁻³ mol.dm⁻³; total Fe concentration in the suspension 2.25 × 10⁻³ mol.dm⁻³. (a) T = 303 K; (b) T = 333 K.

Vegard's law (Cornell and Schwertmann, 1996). However, striking deviation of the a parameter from Vegard's law in the goethite-diaspore solid solution has been reported on many occasions (Schulze, 1984; Schulze and Schwertmann, 1987; Wolska and Schwertmann, 1993). The deviation from the Vegard rule of the a unit-cell edge length is a suitable measure

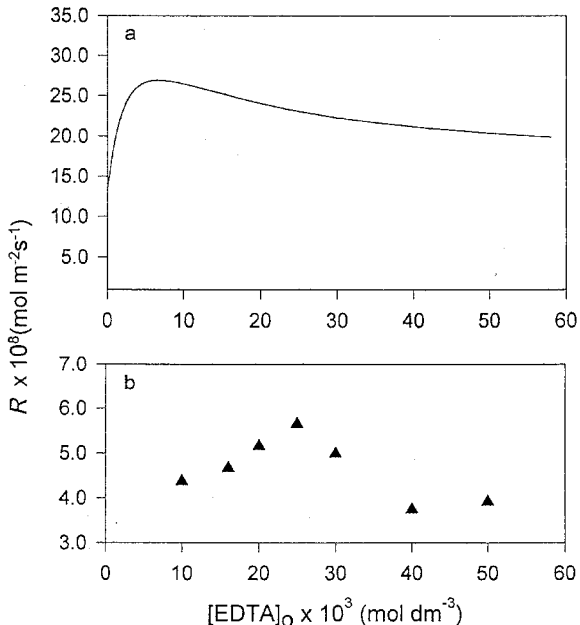


Figure 4. Initial dissolution rates R as a function of [EDTA]. (a) Theoretical model applied to pure goethite. (b) Experimental values for G["]₇ sample; pH 5.5, $T = 303$ K, [S₂O₄²⁻] 5.75 × 10⁻³ mol.dm⁻³, total Fe concentration in the suspension 2.25 × 10⁻³ mol.dm⁻³.

of the number of defects (Schwertmann and Carlson, 1994).

Schwertmann and Carlson (1994) suggested that the lattice parameters are subject to a number of different influences, which may result in similar effects. Besides the incorporation of Al, the changes of the unit-cell dimension may be caused, for example, by the increase in the degree of hydroxylation yielding the defect structures with cation deficiency. Schulze and Schwertmann (1984) concluded that the number of structural defects is greater when the Al content increases and the synthesis temperature decreases.

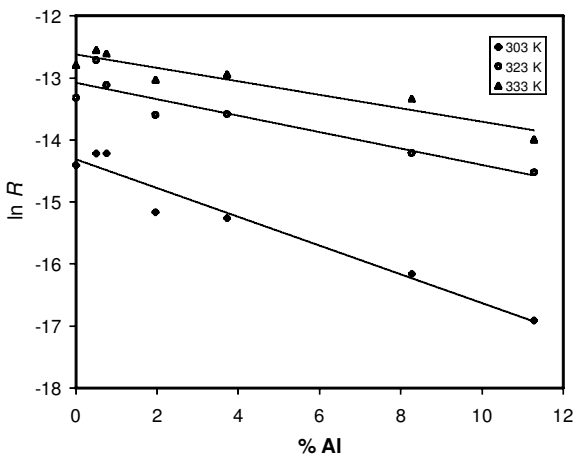


Figure 5. Natural logarithm of R as a function of mol.% Al at three different temperatures; pH 5.5; [EDTA] 0.01 mol.dm⁻³, [S₂O₄²⁻] 5.75 × 10⁻³ mol.dm⁻³, total Fe concentration in the suspension 2.25 × 10⁻³ mol.dm⁻³.

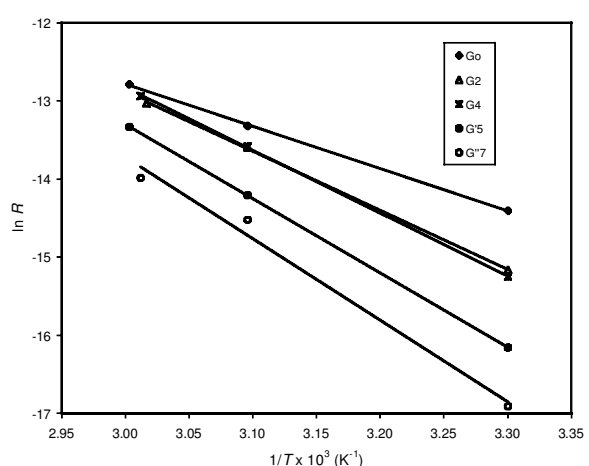


Figure 6. Arrhenius plots for the initial dissolution rates of the different samples. The conditions are specified in Figure 3.

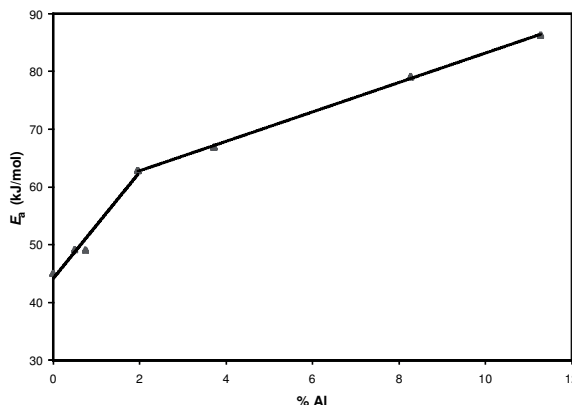


Figure 7. Activation energy as a function of Al content.

On the basis of the characterization of our samples and the synthesis conditions (lower temperatures for higher Al content), and in agreement with the previous statement, a larger number of defects can be expected for more substituted samples.

Although the crystal size decreases and structural defects may increase with the increase of Al substitution, the dissolution rate diminishes.

The relative contribution of two principal pathways of dissolution must be considered here. On the one hand, reduction of Fe^{III} to Fe^{II} destabilizes the coordination sphere of the Fe. Both the loss of charge and the larger size of the bivalent Fe^{II} induce detachment of ions as Fe²⁺. On the other hand, the Al^{III} ion present in the framework of goethite is insensitive to the reductive action of dithionite. Torrent *et al.* (1987) also observed that the initial dissolution rate of goethite in reductive media was depressed with the increase of Al substitution. The same effect was observed in soil goethites (Jeanroy *et al.* 1991).

In accordance with the results reported by Torrent *et al.* (1987) a positive intercept (<5% of total Fe) was observed at 303 K in the kinetic profiles of dissolved Fe fraction *vs.* time in the sample G''₇, where, after 1 h, <50% of the total oxide was dissolved. This sample has a higher Al content and higher amount of oxalate soluble material (Table 1) and this could be attributed to the presence of very small particles. Hence this sample should show an enhanced dissolution and release of Fe at the very beginning. On the other hand, the departures of the linearity could be related to the presence of more amounts of structural defects having more reactive sites.

The kinetic profiles of pure goethite, where the solid phase is totally dissolved, are deceleratory at all temperatures studied. At 303 K, the range of linearity in dissolution plots increases with the increase in the Al substitution. At the same time the fraction of total Fe released from substituted goethite becomes smaller (Figure 3). These results suggest that, for the reductive dissolution of Al-substituted goethites, the detachment of Al is the rate-limiting step.

Table 2. Frequency factor (*A*) and activation energy (*E_a*) derived from the Arrhenius plot for Al-substituted goethites.

Sample	Al substitution (mol.%)	<i>E_a</i> (kJ mol. ⁻¹)	<i>A</i> (mol.m ⁻² s ⁻¹)
G ₀	0	45.03	1.92×10^3
G _m	0.5	49.14	1.27×10^4
G ₁	0.75	49.09	1.06×10^4
G ₂	1.96	62.83	1.06×10^6
G ₄	3.72	66.90	4.87×10^6
G' ₅	8.27	79.11	2.51×10^8
G'' ₇	11.28	86.30	2.18×10^9

Influence of ligand concentration

In the kinetics experiments carried out on pure goethite (Rueda *et al.* 1992), the influence of EDTA at constant pH, reductant concentration, and temperature, was interpreted assuming that the co-adsorption of ligand and dithionite onto vicinal sites promotes dissolution. Three different surface complexes A, B and C, (Figure 8) were required to describe the shape of the kinetic profile in Figure 4a:

The overall rate of dissolution *R* (mol.m⁻²s⁻¹) is then given by:

$$R = k_1 \{A\} + k_2 \{B\} + k_3 \{C\} \quad (1)$$

The braces denote concentration of surface complexes depicted in Figure 8. The monomeric A and C surface species are important at low and high [EDTA]/[D] ratios, respectively. The maximum rate of dissolution observed in Figure 4a is coincident with the maximum in the fraction of dimeric sites B. Data from the total number of surface sites (*N_s*), surface complex constant by EDTA (*K_L*) and ligand and dithionite concentration, must be included in the model. The values of the rate constants, *k₁*, *k₂* and *k₃* associated at the phase transfer of Fe²⁺ from the surface sites A, B and C respectively and the surface complex constant by dithionite (*K_D*) are adjustable parameters. Details of the application of the theoretical model for pure goethite are given in Rueda *et al.* (1992). In the reductive dissolution of goethite in the Fe(II)-EDTA media, the synergistic effect of the ligand adsorbed on vicinal sites was also considered to attain a good fit with the experimental results (Ballesteros *et al.*, 1998).

The low dissolution-rate values observed for the G''₇ sample (Figure 4b) can be attributed to the greater strength of Al-O-Fe bonds relative to the Fe-O bonds. The presence of a flatter and wider maximum in Al-

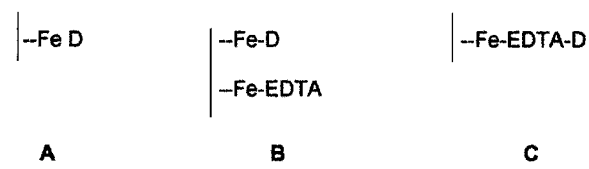


Figure 8. Scheme of the surface complexes considered in the dissolution mechanism.

substituted goethite, could be related in part to the possible decrease in the proportion of dimeric sites with regard to monomeric ones when Al is incorporated into the goethite structure. In this system, the applicability of the model mentioned above is more complex because the constant values K_D and K_L for the surface complexes \equiv Al-EDTA and \equiv Al-D, respectively, must also be included. Besides, the formation of new types of sites with different reactivity and the respective rate constants should be considered.

On the other hand, EDTA concentration affects the Al dissolution through a 'ligand-promoted dissolution mechanism'. Specifically, the ligand-promoted dissolution rate of an oxide is assumed to be directly related to the concentration of 'precursor complexes' on the surface, in such cases:

$$R_L = k_L C_L^s \quad (2)$$

where k_L denotes the ligand-promoted rate constant and C_L^s the sorbed ligand concentration. If sorption of the ligand is fairly weak, C_L^s will be small and a large number of surface sites will be vacant, even when the soluble ligand concentration is large (Lin and Benjamin, 1990). This suggestion agrees with the displacement of the maximum at higher EDTA concentrations observed in Figure 4b.

From the comparison of the ξ potential results for goethite and alumina in the presence of EDTA (Rueda *et al.*, 1985; Bowers and Huang, 1985), we concluded that the affinity of EDTA for the Fe oxide surface is significantly greater than that of the Al oxide surface. These results suggest a low K_L value for the surface complex \equiv Al-EDTA. Generally, the surface complex constant values relate to the values of the constants of complexes in solution. Specifically, K_L is 1.58×10^{15} for Fe(III)-EDTA and 2.51×10^3 for Al(III)-EDTA *i.e.* 12 orders of magnitude smaller. Therefore, Al dissolution is favored with the increase in the soluble EDTA concentration and this is also in agreement with a displacement of the maximum at lower [D]:[EDTA] ratio. These results suggest that at the same time that the Al content increases, the Al transfer phase becomes the predominant pathway in the Al-substituted goethite dissolution.

We can conclude that two different mechanisms must be considered. Iron dissolution includes reduction of the structural metal ion; in such cases dissolution involves the adsorption of reductant, precursor complex formation, electron transfer, release of oxidized adsorbate and the release of reduced structural metal ions (Borghi *et al.*, 1989; Blesa *et al.*, 1994). On the other hand, Al undergoes ligand-promoted dissolution. We found that only <10% of boehmite was dissolved in EDTA-dithionite in the same conditions (unpublished results). Assuming congruent dissolution in Al-substituted goethite, the amount of Al dissolved in pure Al oxide is less than the Al released in the more substituted

goethite (G''_7). It is clear then, that in Al-substituted goethite, the release of Al is improved with regard to pure Al oxide. This improvement occurs due to the relevant Fe atoms in the coordination sphere, which are released. Subsequently, the isolated Al may be transferred to the solution as Al-EDTA complex.

In summary, to achieve a better fit of the experimental values, more free parameters are necessary, but this is unrealistic. Furthermore, the qualitative description, based on the different distribution sites, of the presence of Al, and the difficulty in transferring Al ions from the solid phase to solution, for the reasons mentioned above, explains satisfactorily the shape of the plot of R vs. [EDTA].

Activation energy and frequency factor

The apparent activation energy *vs.* mol.% Al can be fitted easily from two straight lines (Figure 7). The break between the two lines occurs at ~2 mol.% Al substitution. The first, at lower Al substitution, has a sharp slope, which predicts a high increase in E_a with the increase in Al content. This result is in agreement with the drastic changes in the solubility in the reductive media between the isostructural phases goethite and diasporite. The other straight line, with a smoother slope, suggests a more complex dissolution mechanism. The slower slope could be associated with the presence of more structural defects at higher Al content as was previously discussed. The lower synthesis temperatures employed in G'_5 and G''_7 also promote the appearance of structural defects. On one hand, the increase in Al content restrains the dissolution, and on the other, the increase in the number of structural defects acts in the opposite way.

Our results are not in agreement with those reported by Wells *et al.* (2001). They did not find a systematic change in the activation energy of hematites as a function of Al.

An increase in the frequency values as a function of Al substitution is observed in Table 2. These results are also compatible with the presence of more structural defects at greater Al content. Although the frequency factor acts in the opposite sense to the effect of higher activation energy, in the range of the Al substitution studied, it is not sufficient to outweigh the unfavorable effect of the larger activation energy.

In summary, we suggest that at low Al substitution levels (<2 mol.% Al) the arrest in the dissolution kinetic is largely because of the presence of Al. However, at greater levels of Al substitution (>2 mol.% Al) the effect of structural defect partially restrains the Al action and the E_a values obtained were smaller than predicted, in accordance with the slope of the first straight line.

ACKNOWLEDGMENTS

This work was support by CONICET (Argentina) and SGCYT, Universidad Nacional del Sur (Argentina). The

authors acknowledge scientific advice from Dr M.A. Blesa.

REFERENCES

- Ballesteros, M.C., Rueda, E.H. and Blesa, M.A. (1998) The influence of Fe(III) on the kinetics of goethite dissolution by EDTA. *Journal of Colloid and Interface Science*, **201**, 13–19.
- Baumgartner, E., Blesa, M.A., Marinovich, H.A. and Maroto, A.J.G. (1983) Heterogeneous electron transfer as a pathway in the dissolution of magnetite in oxalic acid solutions. *Inorganic Chemistry*, **22**, 2224–2226.
- Blesa, M.A., Morando, P.J. and Regazzoni, A.E. (1994) *Chemical Dissolution of Metal Oxides*. CRC Press, Boca Raton, Florida, Ann Arbor, Michigan, London and Tokyo, 400 pp.
- Borghi, E.B., Regazzoni, A.E., Maroto, A.J.G. and Blesa, M.A. (1989) Reductive dissolution of magnetite by solutions containing EDTA and Fe^{II}. *Journal of Colloid and Interface Science*, **130**, 299–310.
- Bowers, A.R. and Huang, C.P. (1985) Adsorption characteristics of polyacetic amino acids onto hydrous γ -Al₂O₃. *Journal of Colloid and Interface Science*, **105**, 197–215.
- Cambier, P. (1986) Infrared study of goethite of varying crystallinity and particle size. I. Interpretation of OH and lattice vibration frequencies. *Clay Minerals*, **21**, 191–200.
- Cornell, R.M. and Schwertmann, U. (1996) *The Iron Oxides. Structure, Properties, Reactions, Occurrence and Uses*. VCH, Weinheim (Germany), 573 pp.
- Hazemann, J.L., Bérar, J.F. and Manceau, A. (1991) Rietveld studies of the aluminium-iron substitution in synthetic goethite. *Materials Science Forum*, **79–82**, 821–826.
- Jeanroy, E., Rajot, J.L., Pillon, P. and Herbillon, A.J. (1991) Differential dissolution of hematite and goethite in dithionite and its implications on soil yellowing. *Geoderma*, **50**, 79–94.
- Lewis, D.G. and Schwertmann, U. (1979a) The influence of aluminium on the formation of iron oxides: III. Preparation of Al goethites in M KOH. *Clay Minerals*, **14**, 115–126.
- Lewis, D.G. and Schwertmann, U. (1979b) The influence of aluminium on the formation of iron oxides: IV. The influence of [Al], [OH], and temperature. *Clay Minerals*, **27**, 195–200.
- Lim-Nunez, R. and Gilkes, R.J. (1987) Acid dissolution of synthetic metal-containing goethites and hematites. *Proceedings of the International Clay Conference, Denver* (L.G. Schultz, H. van Olphen and F.A. Mumpton, editors). The Clay Minerals Society, Bloomington, Indiana, 197–204.
- Lin, C.F. and Benjamin, M.M. (1990) Dissolution kinetics of minerals in the presence of sorbing and complexing ligands. *Environmental Science Technology*, **24**, 126–134.
- Mann, S., Cornell, R.M. and Schwertmann, U. (1985) High-resolution transmission electron microscopic (HRTEM) study of aluminous goethites. *Clay Minerals*, **20**, 255–262.
- McKeague, J.A. and Day, J.H. (1966) Dithionite and oxalate extractable Fe and Al as aids in differentiating various classes of soils. *Canadian Journal of Soil Science*, **43**, 83–96.
- Mehra, O.P. and Jackson, M.L. (1960) Iron oxide removal from soils and clays by dithionite-citrate system buffered with sodium bicarbonate. *Clays and Clay Minerals*, **7**, 317–327.
- Mendelovici, E., Yariv, S.H. and Villalva, R. (1979) Aluminum bearing goethite in Venezuelan laterites. *Clays and Clay Minerals*, **27**, 368–372.
- Murad, E. and Schwertmann, U. (1983) The influence of aluminium substitution and crystallinity on the Mössbauer spectra of goethite. *Clay Minerals*, **18**, 301–312.
- Norrish, K. and Taylor, R.M. (1961) The isomorphous replacement of iron by aluminum in soil goethites. *Journal of Soil Science*, **12**, 294–306.
- Pollard, R.J., Pankhurst, Q.A. and Zientek, P. (1991) Magnetism in aluminous goethite. *Physics and Chemistry of Minerals*, **18**, 259–264.
- Ruan, H.D. and Gilkes, R.J. (1995) Acid dissolution of synthetic aluminous goethite before and after transformation to hematite by heating. *Clay Minerals*, **30**, 55–65.
- Rueda, E.H., Grassi, R.L. and Blesa, M.A. (1985) Adsorption and dissolution in the system goethite/aqueous EDTA. *Journal of Colloid and Interface Science*, **106**, 243–246.
- Rueda, E.H., Ballesteros, M.C., Grassi, R.L. and Blesa, M.A. (1992) Dithionite as a dissolving reagent for goethite in the presence of EDTA and citrate. Application to soil analysis. *Clays and Clay Minerals*, **40**, 575–585.
- Schulze, D.G. (1984) The influence of aluminum on iron oxides: VII. Unit cell dimensions of Al-substituted goethites and estimation of Al from them. *Clays and Clay Minerals*, **32**, 36–44.
- Schulze, D.G. and Schwertmann, U. (1984) The influence of aluminium on iron oxides: X. Properties of Al-substituted goethites. *Clay Minerals*, **19**, 521–539.
- Schulze, D.G. and Schwertmann, U. (1987) The influence of aluminium on iron oxides: XIII. Properties of goethites synthesized in 0.3 M KOH at 25°C. *Clay Minerals*, **22**, 83–92.
- Schwertmann, U. (1984) The influence of aluminium on iron oxides. IX. Dissolution of Al-goethites in 6 M HCl. *Clay Minerals*, **19**, 9–19.
- Schwertmann, U. and Carlson, L. (1994) Aluminum influence on iron oxides: XVII. Unit-cell parameters and aluminum substitution of natural goethites. *Soil Science Society of America Journal*, **58**, 256–261.
- Schwertmann, U. and Cornell, R.M. (1991) *Iron Oxides in the Laboratory*. VCH, Weinheim, Germany, 137 pp.
- Schwertmann, U. and Latham, M. (1986) Properties of iron oxides in some new Caledonian soils. *Geoderma*, **39**, 105–123.
- Schwertmann, U., Friedl, J., Stanjek, H. and Schulze, D. (2000) The effect of Al on Fe oxides. XIX. Formation of Al-substituted hematite from ferrihydrite at 25°C and pH 4 to 7. *Clays and Clay Minerals*, **48**, 159–172.
- Strauss, R., Brümmer, G.W. and Barrow, N.J. (1997) Effects of crystallinity of goethite: I. Preparation and properties of goethite of differing crystallinity. *European Journal of Soil Science*, **48**, 87–99.
- Torrent, J., Schwertmann, U. and Barrón, V. (1987) The reductive dissolution of synthetic goethite and hematite in dithionite. *Clay Minerals*, **22**, 329–337.
- Wells, M.A., Gilkes, R.J. and Fitzpatrick, R.W. (2001) Properties and acid dissolution of metal-substituted hematites. *Clays and Clay Minerals*, **49**, 60–72.
- Wolska, E. and Schwertmann, U. (1993) The mechanism of solid solution formation between goethite and diaspore. *Neues Jahrbuch für Mineralogie Monatshefte*, 213–233.
- Wolska, E., Szajda, W. and Piszcza, P. (1992a) Determination of solid solution limits based on the thermal behavior of aluminum substituted iron hydroxides and oxides. *Journal of Thermal Analysis*, **38**, 2115–2122.
- Wolska, E., Szajda, W. and Piszcza, P. (1992b) Synthetic solid solutions formed between goethite and diaspore. *Zeitschrift für Pflanzenernährung Düngung und Bodenkunde*, **155**, 479–482.

(Received 4 June 2001; revised 24 January 2002; Ms. 553)